JPE 13-5-15

http://dx.doi.org/10.6113/JPE.2013.13.5.884

Fourier-Based PLL Applied for Selective Harmonic Estimation in Electric Power Systems

Cláudio H. G. Santos*, Reginaldo V. Ferreira**, Sidelmo Magalhães Silva†, and Braz J. Cardoso Filho***

*Dept. of Electronic Eng., Federal University of Ouro Preto (UFOP), João Monlevade, Brazil
**Federal Institute of Minas Gerais (IFMG), Betim, Brazil
†***Dept. of Electrical Eng., Federal University of Minas Gerais (UFMG), Minas Gerais, Brazil

Abstract

In this paper, the Fourier-based PLL (Phase-locked Loop) is introduced with a new structure, capable of selective harmonic detection in single and three-phase systems. The application of the FB-PLL to harmonic detection is discussed and a new model applicable to three-phase systems is introduced. An analysis of the convergence of the FB-PLL based on a linear model is presented. Simulation and experimental results are included for performance analysis and to support the theoretical development. The decomposition of an input signal in its harmonic components using the Fourier theory is based on previous knowledge of the signal fundamental frequency, which cannot be easily implemented with input signals with varying frequencies or subjected to phase-angle jumps. In this scenario, the main contribution of this paper is the association of a phase-locked loop system, with a harmonic decomposition and reconstruction method, based on the well-established Fourier theory, to allow for the tracking of the fundamental component and desired harmonics from distorted input signals with a varying frequency, amplitude and phase-angle. The application of the proposed technique in three-phase systems is supported by results obtained under unbalanced and voltage sag conditions.

Key words: Fourier series, Harmonic detection, Phase-locked loop

I. INTRODUCTION

Shunt and series active filters are important alternatives for compensating the harmonic currents and voltages produced by nonlinear loads. For compensation purposes, a harmonic detection algorithm is expected to supply an estimation of the magnitude, frequency and phase angle of each individual harmonic component. Several techniques and algorithms have been proposed for harmonic detection in active power filtering [1]-[14].

Previous papers on harmonic detection methods differ in terms of their conclusions and recommendations. In [4] Recursive Discrete Fourier Transform (RDFT), Kalman Filter and Instantaneous Reactive Power [5] methods were presented. In [6], the Phase Locked Loop, RDFT and Discrete Kalman Filtering (KFD) methods were compared. Finally, several alternatives were discussed in [7]. These include the adaptive notch filter (ANF), the theory of instantaneous reactive power, synchronous reference, sinusoidal subtraction and the fast Fourier transform. The advantages of each of these methods vary in terms of dynamic response, accuracy, complexity, computational cost, etc.

This paper introduces a new application of the Fourier Based – Phase Locked Loop (FB-PLL) for selective harmonic detection. In a previous paper [8], the FB-PLL was shown to be restricted to the estimation of the fundamental frequency component of three-phase systems. In the present paper, its structure is expanded to allow for harmonic detection in single and three-phase systems. Compared to other methods, the FB-PLL has the advantages of a fast response and simple implementation. It is shown that if the orders of the harmonics in the signal are known, further simplification is possible.

II. PRINCIPLES OF THE FOURIER-BASED PLL

The Fourier Based – PLL (FB-PLL) introduced in [8], is an algorithm based on the Fourier series which is suitable for single-phase systems. An extended version of this PLL algorithm is presented here, covering harmonic estimation in

Manuscript received Apr. 27, 2012; revised Jul. 16, 2013
Recommended for publication by Associate Editor Kyeon Hur.
†Corresponding Author: sidelmo@ufmg.br
Tel: +55-3409-3417, Federal University of Minas Gerais
*Dept. of Electronic Eng., Federal University of Ouro Preto (UFOP), Brazil
**Federal Institute of Minas Gerais (IFMG), Brazil
***Dept. of Electrical Eng., Federal University of Minas Gerais (UFMG), Brazil

single-phase and three-phase systems. In this expanded technique, the Fourier series is used as a tool to allow for the reconstruction of the fundamental frequency of an input signal or any of its harmonic components [9].

It is known that any periodic signal x(t) can be represented by an infinite sum of complex exponential functions, as long as the following conditions are met:

(i) *x(t)* must be absolutely integrable in any period;

(ii) in any finite time interval, *x(t)* should have only limited variations;

(iii) in any time interval, there is only a finite number of discontinuities.

Mathematically, the Fourier series is defined by (1):

$$x(t) = a_0 + \sum_{n=1}^{\infty} \left(a_n \cos(n\omega_0 t) + b_n \sin(n\omega_0 t) \right) \quad (1)$$

where:

$$a_0 = \frac{1}{T_0} \int_{T_0} x(t)\, dt \quad (2)$$

$$a_n = \frac{2}{T_0} \int_{T_0} x(t) \cos(n\omega_0 t)\, dt \quad (3)$$

$$b_n = \frac{2}{T_0} \int_{T_0} x(t) \sin(n\omega_0 t)\, dt \quad (4)$$

where a_0 is the average value of *x(t)*, and a_n and b_n represent the amplitude of the cosine and sine components of the n^{th} harmonic of the periodic signal *x(t)*.

Basically, the Fourier coefficients in (3) to (4) consist of two times the average value of the input signal multiplied by another signal with the frequency of the harmonic of interest and with the magnitude set to one. This interpretation of the Fourier coefficients suggests that the amplitude of the n^{th} harmonic can be computed dynamically.

The main idea of the FB-PLL is the dynamic computation of the Fourier coefficients through a low-pass filters (LPF). To better explain the expanded FB-PLL principle, assume a sinusoidal signal $v_s(t)$ containing several harmonic components (5):

$$v_S(t) = \sum_{n=1,2,\ldots N} V_n \cos(n\omega t + \phi_n) \quad (5)$$

where V_n and ϕ_n are amplitude and phase of the n^{th} harmonic component, and N is the highest order harmonic component used to represent $v_s(t)$.

Suppose that the fundamental frequency of $v_s(t)$ is known, and the amplitude and phase of each of the harmonic components are to be estimated. The first step in the harmonic estimation is the multiplication of $v_s(t)$ by two sinusoidal signals, in quadrature with each other, where both are at the specific harmonic frequency (6), (7):

$$v_{ic}(t) = \cos(H\omega t) \times \left(\sum_{n=1,2,\ldots N} V_n \cos(n\omega t + \phi_n) \right) \quad (6)$$

$$v_{is}(t) = \sin(H\omega t) \times \left(\sum_{n=1,2,\ldots N} V_n \cos(n\omega t + \phi_n) \right) \quad (7)$$

where H is the harmonic order of interest and the sub-indexes *is* and *ic* stand for the *integrand* multiplied by the *sine* or *cosine* terms.

From (7) and (8) and collecting the terms at the harmonic order of interest:

$$v_{ic}(t) = \cos(H\omega t) \times V_H \cos(H\omega t + \phi_H) + \ldots \\ \ldots \cos(H\omega t) \times \left(\sum_{n=1,2,\ldots H-1,H+1,\ldots N} V_n \cos(n\omega t + \phi_n) \right) \quad (8)$$

$$v_{is}(t) = \sin(H\omega t) \times V_H \cos(H\omega t + \phi_H) + \\ \ldots \sin(H\omega t) \times \left(\sum_{n=1,2,\ldots H-1,H+1\ldots N} V_n \cos(n\omega t + \phi_n) \right) \quad (9)$$

In (8) and (9), the term $V_H cos(H\omega t+\phi_H)$ can be substituted by $a_H cos(H\omega t)+b_H sin(H\omega t)$, leading to (10), (11):

$$v_{ic}(t) = \cos(H\omega t) \times \left(a_H \cos(H\omega t) + b_H \sin(H\omega t) \right) + \ldots \\ \ldots \cos(H\omega t) \times \left(\sum_{n=1,2,\ldots H-1,H+1,\ldots N} V_n \cos(n\omega t + \phi_n) \right) \quad (10)$$

$$v_{is}(t) = \sin(H\omega t) \times \left(a_H \cos(H\omega t) + b_H \sin(H\omega t) \right) + \ldots \\ \ldots \sin(H\omega t) \times \left(\sum_{n=1,2,\ldots H-1,H+1,\ldots N} V_n \cos(n\omega t + \phi_n) \right) \quad (11)$$

Applying the properties of trigonometric functions, it can be shown that:

$$v_{ic}(t) = \frac{a_H}{2} \left(1 + \cos(2H\omega t) \right) + \frac{b_H}{2} \sin(2H\omega t) + \ldots \\ \ldots \cos(H\omega t) \times \left(\sum_{n=1,2,\ldots H-1,H+1,\ldots N} V_n \cos(n\omega t + \phi_n) \right) \quad (12)$$

$$v_{is}(t) = \frac{b_H}{2} \left(1 - \cos(2H\omega t) \right) + \frac{a_H}{2} \sin(2H\omega t) + \ldots \\ \ldots \sin(H\omega t) \times \left(\sum_{n=1,2,\ldots H-1,H+1,\ldots N} V_n \cos(n\omega t + \phi_n) \right) \quad (13)$$

From equations (12) and (13), it can be seen that $v_{ic}(t)$ and $v_{is}(t)$ have dc components with magnitudes of $a_H/2$ and $b_H/2$, respectively. Therefore, the amplitudes a_H and b_H, of signals $v_{is}(t)$ and $v_{ic}(t)$ can be obtained through a Low Pass Filter (LPF). These two signals can be divided into two components, dc and ac, as follows:

$$v_{ic} = \overline{v}_{ic} + \tilde{v}_{ic} \tag{14}$$

$$v_{is} = \overline{v}_{is} + \tilde{v}_{is} \tag{15}$$

where $\overline{v}_{ic}$ denotes the dc component and $\tilde{v}_{ic}$ denotes the ac component of v_{ic}. Thus $\overline{v_{ic}} = a_H / 2$ and $\overline{v_{is}} = b_H / 2$. The ac components are:

$$\tilde{v}_{ic} = \frac{a_H}{2}\cos(2H\omega t) + \frac{b_H}{2}\sin(2H\omega t) + \ldots \\ \ldots\cos(H\omega t)\times\left(\sum_{n=1,2,\ldots H-1,H+1,\ldots N} V_n \cos(n\omega t + \phi_n)\right) \tag{16}$$

$$\tilde{v}_{is} = -\frac{b_H}{2}\cos(2H\omega t) + \frac{a_H}{2}\sin(2H\omega t) + \ldots \\ \ldots\sin(H\omega t)\times\left(\sum_{n=1,2,\ldots H-1,H+1,\ldots N} V_n \cos(n\omega t + \phi_n)\right) \tag{17}$$

Equations (16-17), show that the signals $\tilde{v}_{ic}$ and $\tilde{v}_{is}$ have components with twice the frequency of the harmonic of interest, and the amplitudes of these components are $a_H/2$ or $b_H/2$. Assuming that these amplitudes are estimated by the filtering signals $v_{ic}(t)$ and $v_{is}(t)$, it is then possible to reconstruct the components in v_{ic} and v_{is}, with a frequency of $2H\omega$. These reconstructed signals can be used in a feedback loop to reduce the amplitude of the components at a frequency of $2H\omega$, thus improving the filtering. This process is presented here in a structure that comprises Eqs. (6-17), referred to as the denominated *Dynamical Fourier Analysis* (DFA). Note that the term $-b_H/2\cos(2H\omega t)$ shows up in the block diagram as a positive feedback (as shown in fig. 1), since its signal in eq. (17) is negative.

In order to eliminate the other harmonic components ($n = 1,2,\ldots H-1,H+1,\ldots N$), it is proposed that the DFA be used for each harmonic of interest and the estimated values should be subtracted to obtain a clean input for the respective DFA block. The estimated signals are reconstructed using the Original Signal Reconstruction block (OSR). A DFA block in series with an OSR block is the denominated Dynamic Fourier Synthesis (DFS).

The DFA block is illustrated in fig. 1 (a). Fig. 1 (b) shows the OSR block used to build the estimated harmonic component with the amplitude and phase information. To obtain the frequency component of interest, sine and cosine multiplications are required. The generation of these two signals requires phase information, which is estimated using a Phase Detector (PD). This is typical of many PLL methods [2]-[14], as shown in fig. 2.

The Fourier synthesis is performed using the sum of all the estimated components, i.e. the output of each OSR, as shown in fig. 3. Each DFA and OSR pair is set for a specific

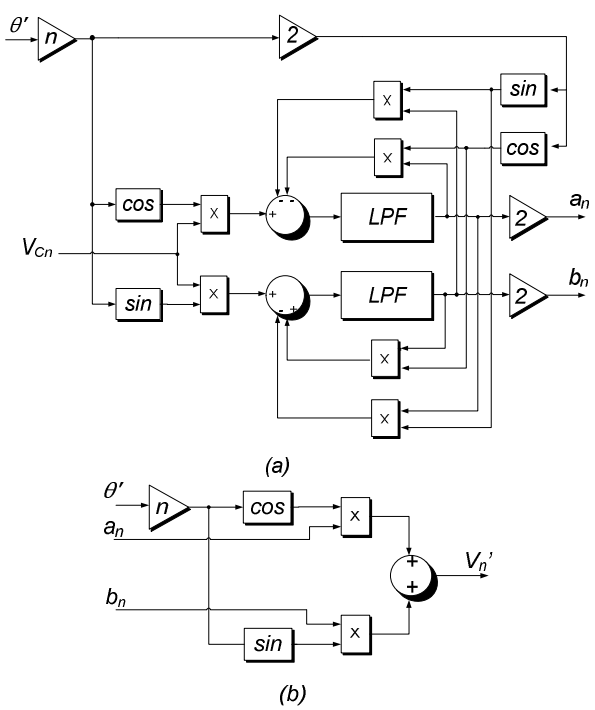

Fig. 1. (a) Dynamic Fourier analysis (DFA); (b) Original Signal Reconstruction (OSR).

harmonic. To provide a clean signal for each DFA analysis, the output of the other harmonics OSRs are subtracted from the input signal, giving each DFA a clean signal denoted as V_{Cn}, where n stands for the harmonic order.

It is important to point out that the FB-PLL structure drawn in fig. 3 includes only the 1st, 3rd and 5th harmonics for a single-phase distorted input. However, the structure can be expanded, for example to the 7th harmonic by adding another DFA/OSR pair, set for this frequency. The number and order of the harmonics to be extracted from the input signal is defined based on the application requirements.

Fig. 1(a) shows that the input signal is multiplied by sine/cosine signals before it is fed to a dynamic average calculator. The average value of these multiplications is extracted with a LPF, implemented in the frequency domain using eq. (18) and a nonlinear feedback.

$$LPF = \frac{1}{\tau s + 1} \tag{18}$$

The sine and cosine terms with doubled frequency act as non-linear feedback gains to eliminate the alternate components. Phase θ' is obtained through a phase detector, based on a PI controller that uses the error between the estimated signal and the input signal to calculate the fundamental frequency. Gain n defines which harmonic will be analyzed. As outputs, for each harmonic component, the coefficients a_n and b_n, shown in eq. (1), (3) and (4), are expected.

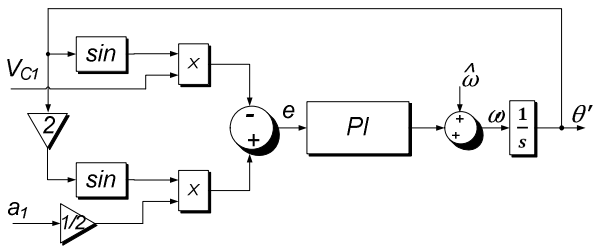

Fig. 2. Phase detector schematic diagram.

With phases and harmonic magnitudes available, the OSRs output the terms in the Fourier Series, taking a_n, b_n and angle θ' as input parameters. Gain n is also used to define the harmonic order in the OSR block.

Fig.2 illustrates a schematic diagram of the phase detector used to estimate the phase angle of the fundamental component. Signal V_{C1} is the input after the removal of all the harmonic content considered in the algorithm, while a_1 is the amplitude of the fundamental component. Using these two signals, the algorithm calculates the phase error, defined by eq. (19), which is taken as the input of the *PI* controller. When the FB-PLL algorithm converges ($a_1 cos(\theta') \approx V_{C1}$), the error tends to zero.

$$e = \frac{a_2}{2}\sin(2\theta') - V_{C1}\sin(\theta') \tag{19}$$

The output of the *PI* block added to the initial value defined for the angular frequency is the estimated fundamental frequency value (ω'). An integrator transforms ω' in the estimated phase angle (θ').

III. Design of the Phase Detector

In this section, the design of the parameters of the FB-PLL is briefly explained. Basically, these parameters are the proportional gain (K_p), the integral gain (K_i) and the time constant (τ) of the first order *LPF*. The design procedure is based on [11], in which a linear model was introduced to represent the phase detection algorithm.

Fig. 4 (a) shows a linear model of the phase detector. In this model, the actual phase is the input and the estimated phase is the output. The error applied to the *PI* controller is the phase error multiplied by the input amplitude, which corresponds to the frequency estimation. Integrating the frequency estimation, one obtains the estimated phase.

The transfer functions relating the phase and the phase error with the input signal are given as:

$$\frac{\Theta'(s)}{\Theta(s)} = \frac{V_P(K_P s + K_I)}{s^2 + V_P K_P s + V_P K_I} \tag{20}$$

and:

$$\frac{E(s)}{\Theta(s)} = \frac{s^2}{s^2 + V_P K_P s + V_P K_I} \tag{21}$$

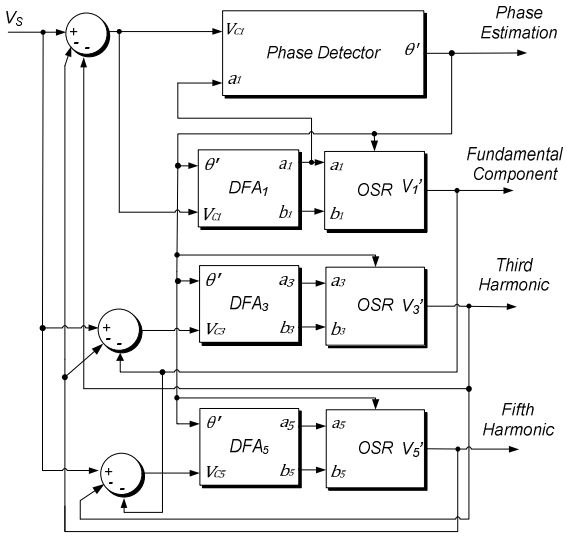

Fig. 3. Fourier Based PLL block diagram considering 1st, 3rd and 5th harmonic components.

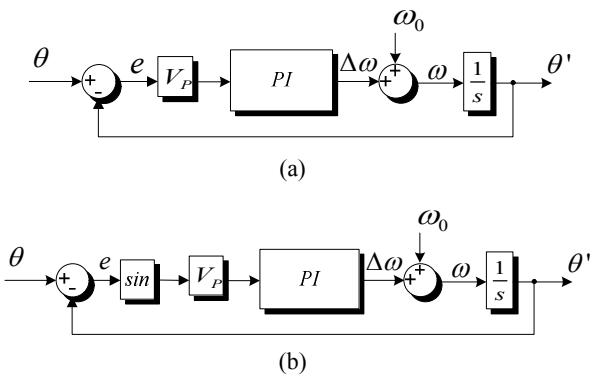

Fig. 4. Phase Detector models: (a) equivalent linear model, (b) actual nonlinear model.

Since this is a second order system, it can be stated that the damping coefficient (ξ) and the cutting frequency (ω_C) are given by:

$$\xi = \frac{K_P}{2}\sqrt{\frac{V_P}{K_I}} \tag{22}$$

and:

$$\omega_C = \sqrt{K_I V_P} \tag{23}$$

Since the linear model of the phase detector is a second order system, its minimum cost for transient settling is achieved when the coefficient ξ is equal $\sqrt{2}$ [11]. Based on the latter reference, the frequency ω_C is considered to be 2.5 times smaller than the input frequency. Finally, the chosen values for ω_C and ξ, assuming a system with a 180V amplitude and a 60Hz fundamental frequency, are presented in Table I. The chosen time constant τ is also presented in the same table. All of the simulations and experimental results included in this paper consider the parameters set to the values pointed out in

TABLE I
GAINS APPLIED IN THE FB-PLL.

Parameter	Value	Unit
K_I	126.33	rad/V
K_P	2.36	rad/Vs
$\tau_{(LPF)}$	23.60	ms

Table I.

In order to make a comparison between the linear and the actual nonlinear phase detector models, shown in fig. 4 (b), simulations of both models were made considering the parameters in Table I. The response of the linear and the nonlinear models of the systems are presented in fig. 5, (a) and (b), respectively. These figures show the *xy* plot of the estimated frequency as a function of the phase error for several initial phase values ($-\pi$, $-\pi/2$, 0, $+\pi/2$ and $+\pi$), which are represented by circles.

As it can be seen, both systems converge, reaching 377rad/s and zero phase error. In addition, although nonlinear in nature, the actual PD converges faster and with a smaller error than the linear model.

Another parameter of concern is the first order *LPF* time constant τ. The use of a 1st order *LPF* is not sufficient to completely eliminate the oscillatory components resultant from the sine and cosine multiplications. Therefore, the ac component is actually eliminated by a nonlinear feedback action, as explained previously.

IV. SIMULATION RESULTS FOR SINGLE PHASE SYSTEMS

This section presents the performance of the single-phase FB-PLL for the fundamental frequency tracking capability and harmonic decomposition performance.

A. Tracking Capability

This simulation illustrates the tracking response characteristics of the FB-PLL. For this simulation, an input signal containing 1p.u. of fundamental frequency (60Hz), 0.2p.u. of the fifth harmonic and 0.3p.u. of the seventh harmonic was used. The amplitude of the fundamental component of the signal was set to 180V. Fig. 6 shows the tracking performance for the fundamental frequency of the FB-PLL.

Fig.7 shows the percentage error of the single-phase FB-PLL algorithm over time. It is observed that the oscillations decrease to less than 5% in approximately 35ms.

B. Harmonic Decomposition Capability

To check the capability of the harmonic decomposition of the algorithm, a signal with a sudden change in the amplitude of the fundamental and harmonic components was applied. The signal is initially composed of 1 p.u. of the fundamental frequency, 0.1 p.u. of the fifth harmonic and 0.4 p.u. of the seventh harmonic. After the variation in the amplitude, the fundamental component is changed to 1.2 p.u., the fifth

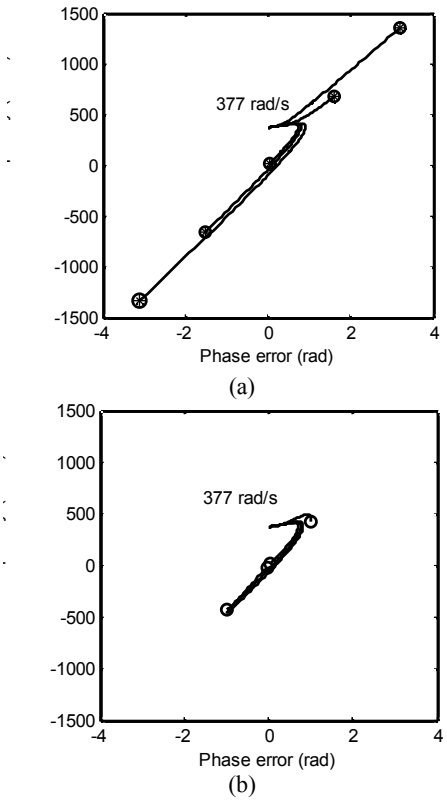

Fig. 5. Phase detector convergence results. (a) linear model; (b) actual nonlinear model.

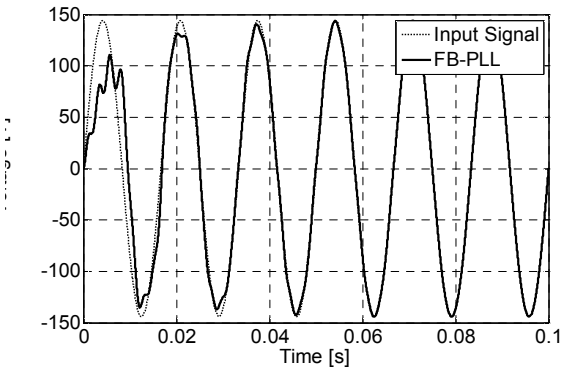

Fig. 6. Response of the Single-Phase FB-PLL model compared with the expected fundamental signal.

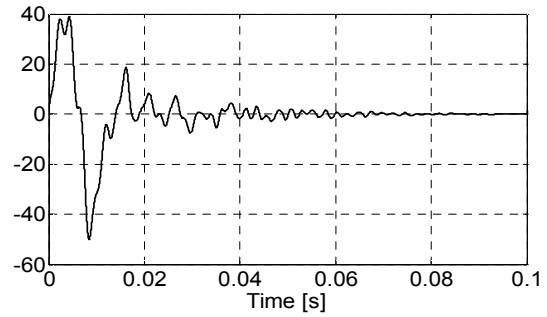

Fig. 7. Percentage error of the single-phase FB-PLL over time.

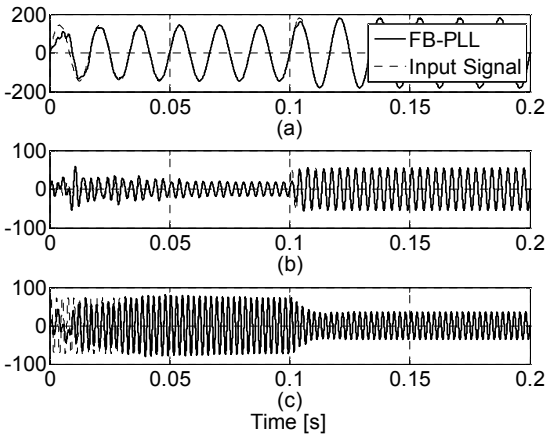

Fig. 8. Harmonic decomposition performed by the FB-PLL in the presence of a change in amplitude.

harmonic to 0.2p.u., and the seventh harmonic to 0.2p.u.

Fig. 8 shows the simulation results, where the fundamental component is seen in fig. 8 (a), the fifth harmonic in fig. 8 (b), and the seventh harmonic in fig. 8 (c). In the fundamental frequency plot, it is observed that the algorithm quickly tracks the input signal, with amplitude oscillations lasting for less than half a cycle. For the fifth and seventh harmonics, the oscillations have a longer duration in terms of number of cycles, but in all cases the error in the steady state is zero.

V. THREE-PHASE APPLICATIONS

The structure of the FB-PLL adapted for three-phase systems can be seen in fig. 9. In this case, the voltages v_a, v_b and v_c go through a Clarke transformation, and are then fed into the Dynamic Fourier Synthesis (DFS). The Clarke transformation is implemented through eq. (11) and (12), where V_{abc} is a vector with the phase voltages, and $V_{\alpha\beta 0}$ indicates the alpha, beta and zero sequence components.

$$V_{\alpha\beta 0} = K_S V_{abc} \tag{24}$$

$$K_S = \frac{2}{3}\begin{bmatrix} 1 & -\frac{1}{2} & -\frac{1}{2} \\ 0 & -\frac{\sqrt{3}}{2} & \frac{\sqrt{3}}{2} \\ \frac{1}{\sqrt{2}} & \frac{1}{\sqrt{2}} & \frac{1}{\sqrt{2}} \end{bmatrix} \tag{25}$$

The use of the Clarke transformation for three-phase systems separates the zero sequence components from the positive and negative sequence components. Since the α and β components include only positive and negative sequence components, like the 7th and 5th, and the *0*-sequence components comprehend the integer multiples of the 3rd harmonic, the DFS for the α and β components have to take into account only the positive and negative sequences, while

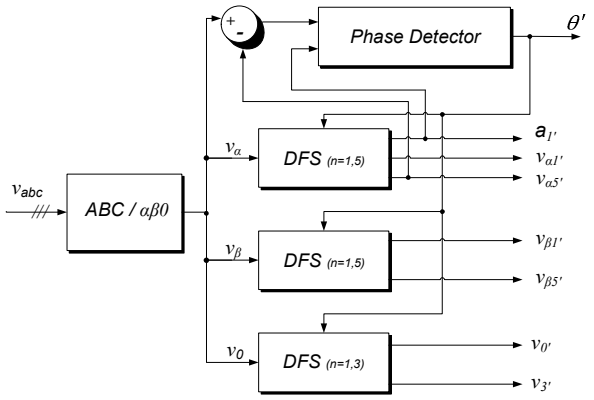

Fig. 9. Structure of the FB-PLL to estimate the 1st, 3rd and 5th harmonics.

the *0*-sequence has to deal only with the zero sequence components.

In three-phase grids with no neutral conductor (three-phase three-wire systems) it is not necessary to consider zero sequences harmonics in the algorithm. Therefore, the three-phase FB-PLL becomes simpler to implement using the Clarke transformation.

The individual DFS blocks for the α and β components are identical and must be able to extract the positive and negative sequence harmonic components immersed in the input signal. The DFS for the zero sequence components needs to be able to extract only the triple harmonics.

This algorithm can also be used for unbalanced system estimation with zero steady state error. Since the DFS blocks are decoupled from each other, it is not necessary for the α and β components to have the same amplitudes. The amplitude difference is a result of the fundamental negative sequence present in the system. Thus any fundamental unbalance is handled by this approach.

VI. SIMULATION RESULTS FOR THREE-PHASE SYSTEMS

In this section, simulation results of the FB-PLL are presented and analyzed. The parameters used for these simulations are listed in Table I.

Fig. 10 shows the operation of the FB-PLL for a three-phase ideal sinusoidal input signal with an amplitude set to 180V and a fundamental frequency set to 60Hz. As can be seen, the estimated frequency and amplitude stabilize at approximately 377rad/s and 180V, respectively. The estimated phase angle is also shown in this figure.

Fig. 11(a) shows the FB-PLL performance under a 30% frequency variation, which is over and under the rated value. Although the estimated frequency oscillates during the transient settling time, the accommodation occurs at around a cycle period. This is seen as good performance when compared to other PLL methods [8]. Fig. 11(b) shows the FB-PLL behavior assuming a sudden 30° phase shift. As can be seen,

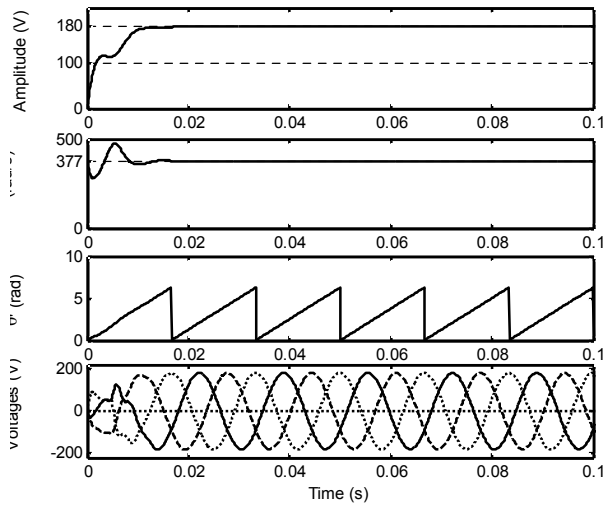

Fig. 10. Operation of the three-phase FB-PLL for an ideal input signal.

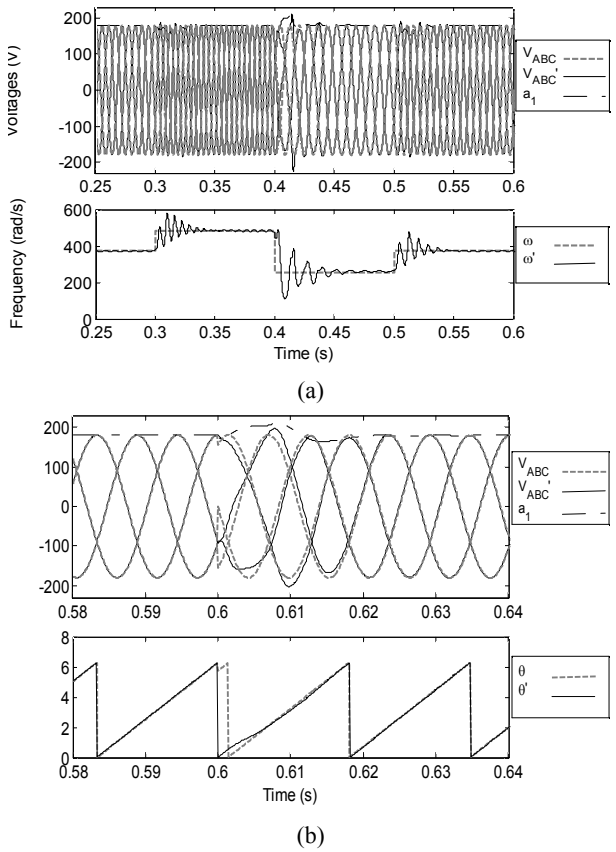

Fig. 11. FB-PLL performance under: (a) 30% frequency variation; (b) phase shift.

the estimated phase tracks the input phase in one cycle, which is a good result when compared to other PLL methods.

Fig. 12 shows the operation of the FB-PLL during different types of amplitude variations. In these figures, the input signal is compared with the estimated signal and its estimated amplitude. In fig. 12 (a), the response of the system for a 50%

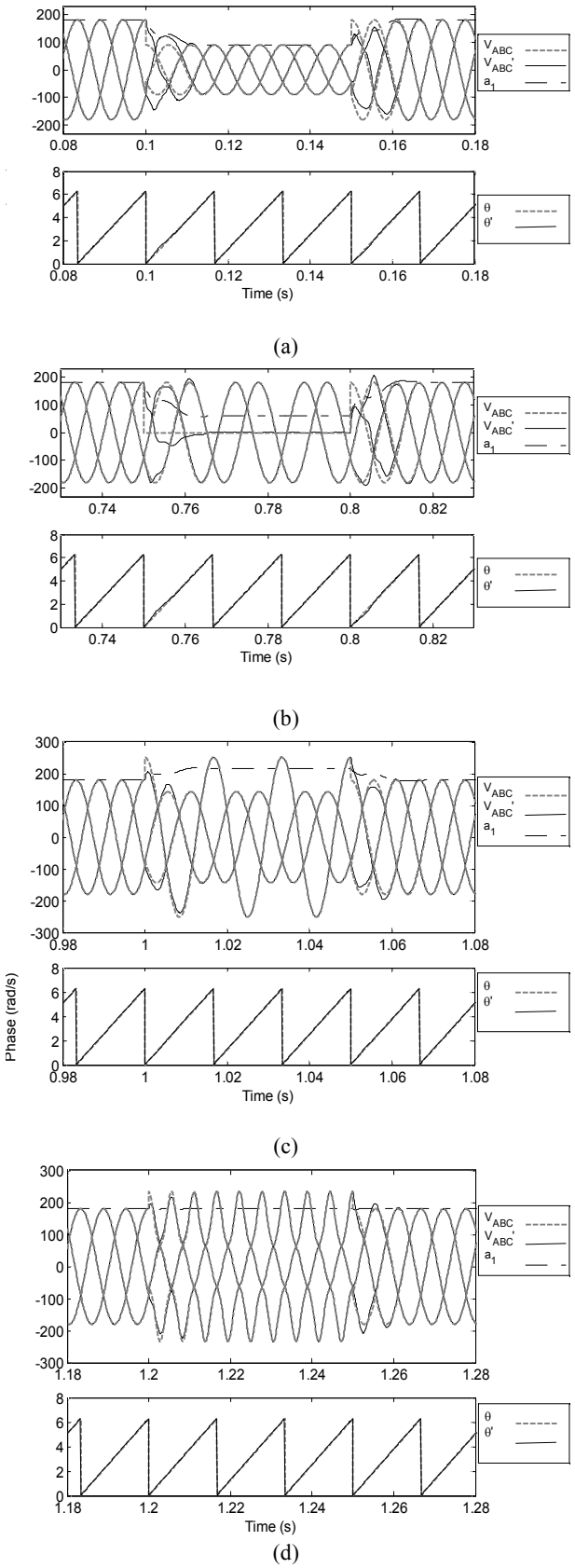

Fig. 12. FB-PLL performances during different types of disturbances: (a) 50% three phase voltage sag; (b) single-phase voltage interruption, (c) voltage unbalance; (d) fifth harmonic distortion.

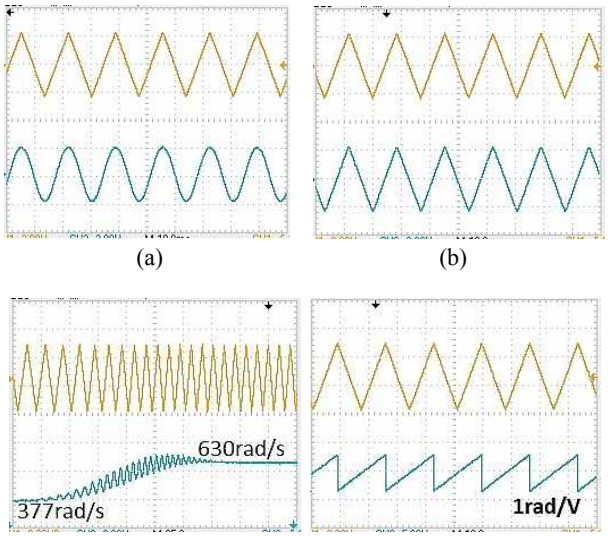

Fig. 13. Experimental results of the FB-PLL for a single-phase triangular signal from function generator: (a) Triangular input and fundamental; (b) Input and signal reconstructed; (c) Input and frequency; (d) Input and phase.

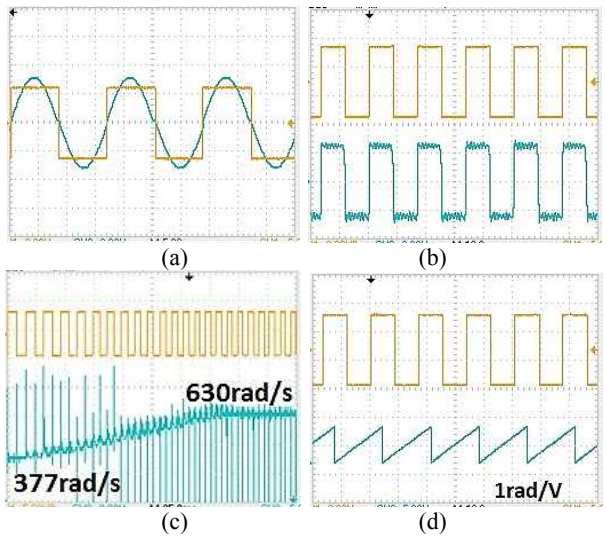

Fig. 14. Experimental results of the FB-PLL for a single-phase square signal from function generator: (a) Square input and fundamental; (b) Input and signal reconstructed; (c) Input and frequency; (d) Input and phase.

three-phase voltage sag with a *50ms* time duration is presented. Notice that the tracking time is approximately half a cycle, due to the use of the LPF. Fig. 12 (b) shows the performance of the FB-PLL for a single-phase voltage interruption on phase *A*. In this kind of sag, negative and zero sequence components are present. No disruption in the operation of the algorithm is observed. A similar result is presented in fig. 12 (c), in which an unbalanced fault is applied. Fig. 12 (d) shows the performance during the presence of the fifth harmonic distortion. As shown, the fundamental amplitude estimated by the PLL remains almost unchanged by the harmonic content. In fig. 12 (b-d), the estimated phase angle is compared with the actual phase angle. It is shown that the tracking capability is not disturbed by the occurrence of these disturbances. This feature is extremely important for power electronic systems which are dependent on phase control, or require synchronization with a power grid.

VII. Experimental Results

In this section, experimental results are shown to confirm the performance of the FB-PLL under many different conditions. In the first set of results, triangular and square wave signals are used as inputs to the system. The selected harmonics for analysis are the 1st, 3rd, 5th, 7th, 9th, 11th, 13th, 15th, 17th and 19th. The second experiment is the harmonic selective detection from a three-phase rectifier input current. In this case, the selected components for detection are 1st, 5th, 7th, 11th, 13th, 17th and 19th. All of the experimental results are presented as screenshots from an oscilloscope. The scales are detailed in the pictures, e.g. V/rad, for phase, and V/A for current.

Fig. 13 shows the results with a triangular waveform as the input of the FB-PLL. Fig. 13 (a) shows the upper input signal compared with the lower estimated fundamental. This seems to agree with the expected sinusoidal waveform in phase with the input. In fig. 13 (b) the upper input signal is compared with the summation of all the estimated harmonics. As can be noticed, the signals are very similar in terms of shape and phase, as expected. Fig. 13 (c) shows the performance of the FB-PLL under a slow frequency variation, with the input in the upper part and the estimated frequency in the lower part. As can be observed, the frequency is well estimated, although with some oscillation during the transient. Fig. 13 (d) shows the estimated phase angle under the same conditions.

Fig. 14 shows similar results as fig. 13, except that the input is a square wave. Fig. 14 (b) shows the sum of all estimated components (bottom signal) compared with the input (top signal). It is shown that the estimated signal is similar to the input signal, except for the fact that it oscillates during sudden changes. Fig. 14 (c) shows the estimated frequency (bottom signal) under a slow frequency variation of the input (top signal). Although it presents some spikes, the frequency converges, and after integration delivers an adequate estimation of the phase angle, as observed in fig. 14 (d).

In another experiment, a three-phase full-bridge rectifier is used to feed the dc side with a parallel capacitor/resistor load, as shown in fig. 15. A capacitor Cd (170 μF) is added to reduce the dc voltage ripple, and the resistor Rload (220Ω) is the rectifier load. The current IL is measured through a

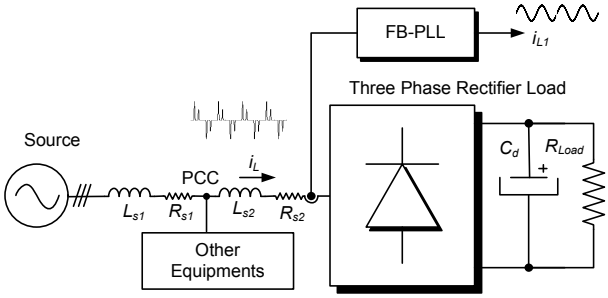

Fig. 15. Experiment setup for the three-phase rectifier.

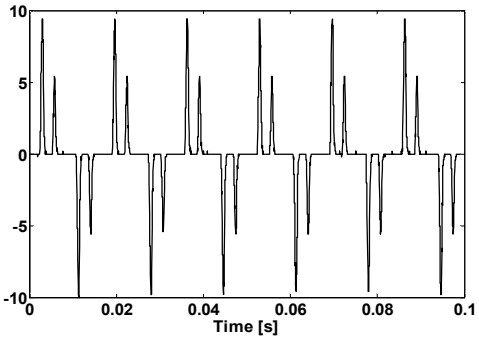

Fig. 16. Current signal measure in the experiment.

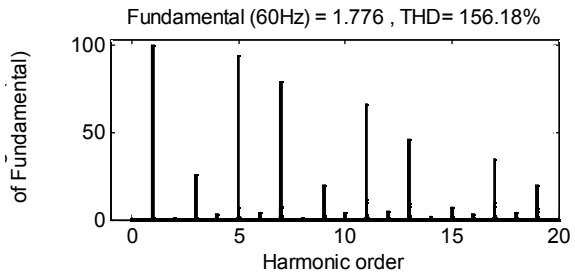

Fig. 17. Frequency spectrum of the distorted current of the rectifier.

current transformer and taken to the input of the FB-PLL for detection of the harmonic components in this signal, as illustrated in fig. 15.

Fig. 16 presents a waveform of the measured current of the rectifier. The spectrum of this signal is shown in fig. 17 and it shows the presence of all the analyzed harmonics.

In fig. 18 (a), the actual input signal (top) is shown to be in phase with the estimated fundamental component (bottom). As observed, the estimated fundamental signal is in phase with the FB-PLL input.

Fig. 18 (b) shows a comparison between the input signal (top) and the summation of all the estimated components (bottom). As can be seen, a good agreement has been achieved. Table II presents the percentage error of the peak value for each analyzed component. This table shows that the highest frequency harmonic has the most significant

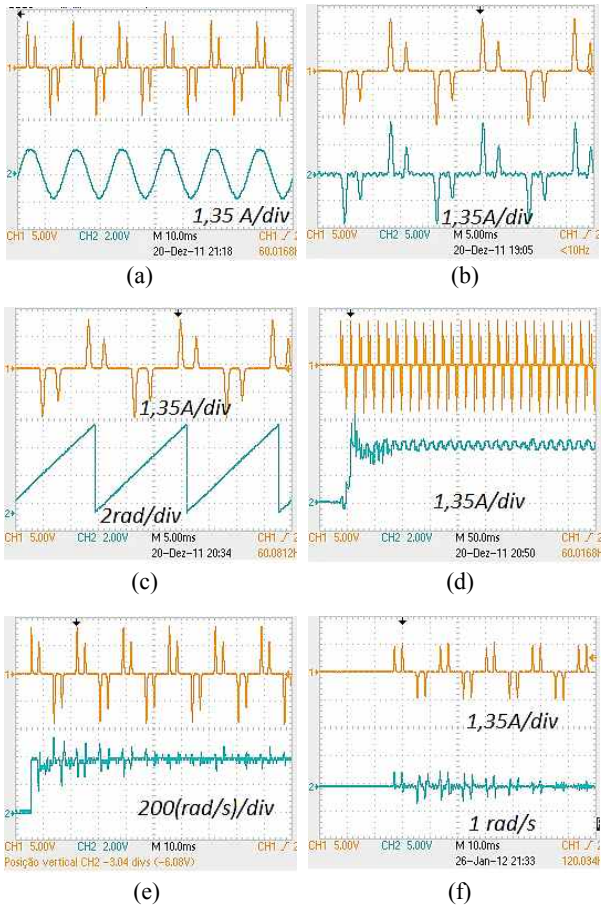

Fig. 18. Experimental results of the FB-PLL for the three-phase rectifier. Input signal with (a) estimated fundamental component; (b) reconstructed signals; (c) estimated fundamental angle; (d) estimated fundamental amplitude; (e) fundamental frequency; (f) phase error.

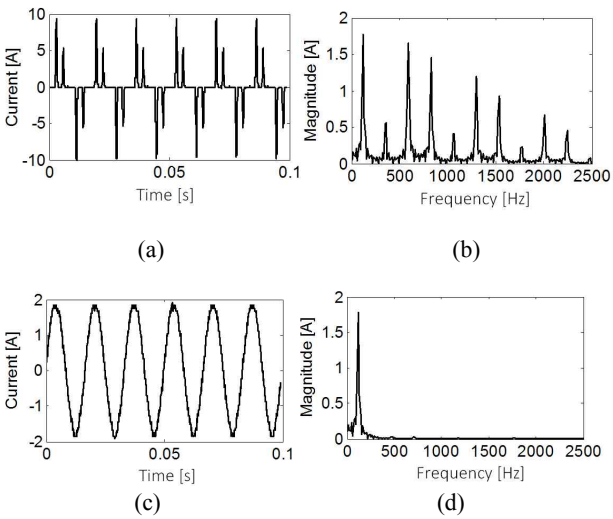

Fig. 19. (a) Original current signal; (b) Frequency spectrum of signal “a”; (c) Estimated fundamental component; (d) Frequency spectrum of signal “c”.

TABLE II
HARMONIC COMPONENTS ESTIMATION. PEAK PERCENTAGE MAGNITUDES FROM 1ST TO 19TH ORDER.

Harmonic Order	Original Signal Magnitude [%]	Estimated Signal Magnitude [%]	Error [%]
1º	52,79	52,75	0,08
5º	50,71	50,65	0,12
7º	45,21	45,81	1,31
11º	39,75	39,05	1,79
13º	31,30	31,81	1,60
17º	24,39	23,50	3,79
19º	16,53	19,72	16,18

estimation error. This is due to the fact that they are closer to the harmonics not selected for analysis. However, it is clear that for the fundamental and low order harmonics, the estimation is close to the actual content, within a 2% error.

Fig. 18 (c) shows the estimated phase practically undisturbed by the harmonics and tracking the phase of the input signal. Fig. 18 (d-f) shows the tracking transients in the amplitude, frequency and phase error. The tracking transient is reasonably fast. Faster convergence can be achieved if a smaller number of harmonics are analyzed.

A comparison of the frequency spectrums of these two signals is shown in fig. 19. As observed, the technique produces a clean fundamental component.

This method presents good performance in both single-phase and three-phase applications. This is supported by simulation and experimental results. Even under high harmonic distortions, unbalance, amplitude, frequency and phase variation, the method continues to track the input signal with a fast response.

VIII. COMPARISON WITH OTHER METHODS

In this section, the FB-PLL is compared with two other methods available in the literature. The Adaptive Notch Filter (ANF) in [14] and the Double Synchronous Reference Frame PLL (DSRF-PLL) in [10], [11]. The comparison is made through simulation results of the techniques under the same type of disturbance. The simulations were implemented in MATLAB®Simulink and the parameters used in each simulation were set aiming for the best performance under each situation.

To analyze the FB-PLL performance under harmonic distorted inputs, it will be compared with the ANF assuming the presence of the 5th and 7th harmonic components. The ANF is an Adaptive filter designed for static converter control purposes, and aiming for selective harmonic compensation. The authors of [14] show the capacity of this method to track distorted signals under the frequency, phase and amplitude of fundamental and harmonic variations. Fig. 20 shows the simulation results of both techniques with the same input, a 10V disturbed signal with 5th and 7th harmonics that vary at instant 0.5s. As can be seen, both methods show similar performances. In the estimation error, which is the difference between the actual input (*Vs*) and the estimated input (*Vs'*), the FB-PLL presents a larger error during the transient, but also a shorter settling time.

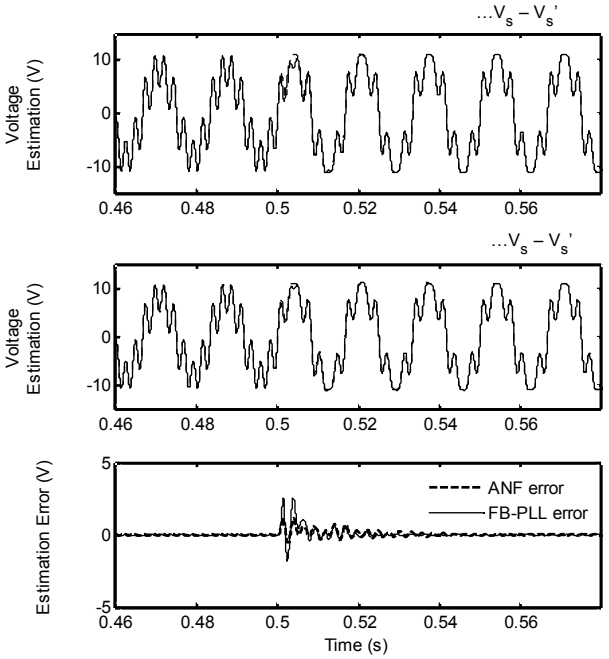

Fig. 20. Comparison between FB-PLL and ANF single-phase input estimations under variable harmonic content. Vs – Vs'.

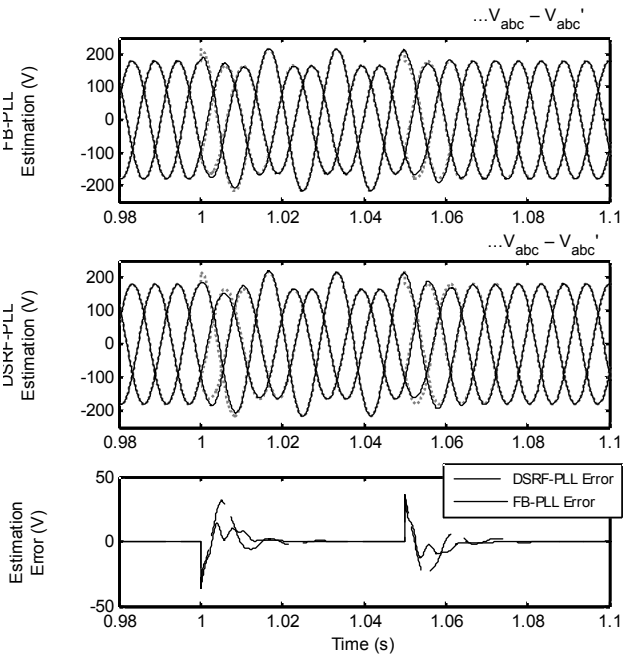

Fig. 21. Comparison between FB-PLL and DSRF-PLL input estimations under three-phase voltage unbalance.

To analyze the performance under a voltage unbalance, the

FB-PLL is compared to the DSRF-PLL, a method introduced in [10] that proposes a double synchronous reference frame for three-phase unbalanced systems with negative and positive sequences. The basic idea of this method is to synchronize the three-phase unbalanced signals using one reference frame for the positive sequence and another frame for the negative, along with subtracting the mutual disturbance between each frame. Fig. 21 shows the simulation results for both methods with the same unbalanced disturbance at the input, starting at 1s and finishing at 1.05s. The amplitude of the input signal is 180V. For this situation, both methods present similar performances, only differing in the initial error during the variation, which is smaller in the FB-PLL.

IX. CONCLUSIONS

In this paper, a Fourier-based PLL technique is shown in an expanded version applied for selective harmonic estimation and three-phase applications. The main principle of this method is to realize the Fourier analysis dynamically by means of a filter structure capable of calculating the average value of a signal with small steady state error. To operate the PLL, phase information is obtained using a phase detector typical of many PLL methods. The theoretical development presented is based on the Fourier analysis and synthesis. A brief convergence analysis of the phase detector is presented to justify the design of the PLL parameters. The results for single-phase and three-phase distorted signals are shown. In these results, the FB-PLL is shown to be suitable for harmonic detection in the presence of voltage sag, frequency variation, unbalance, phase-shift and harmonic distortion. Experimental results give practical support for the theoretical development and simulation results. The FB-PLL shows a clean spectrum of the estimated fundamental component. A comparison with two other methods, the ANF and the DSRF-PLL was conducted. These results show that the FB-PLL has performance that is similar to these methods.

This paper has successfully extended the application of the FB-PLL to three-phase systems and it presented simulation and experimental results that support the theoretical development. The ability of this technique to correctly estimate phase and frequency information from voltage and currents signals under many different kinds of disturbances has been demonstrated.

REFERENCES

[1] P. Mattavelli, "A closed-loop selective harmonic compensation for active filters," *IEEE Trans. Ind. Appl.*, Vol. 37, No. 1, pp. 81-89, Jan./Feb. 2001.

[2] L. Asiminoaei, F. Blaabjerg, and S. Hansen, "Detection is key – harmonic detection methods for active power filter applications," *IEEE Ind. Appl. Mag.*, Vol. 13, No. 4, pp. 22-33, Jul./Aug. 2007.

[3] D. Yazdani, A. Bakhshai, G. Joos, and M. Mojiri, "A real-time three-phase selective harmonic extraction approach for grid-connected converters," *IEEE Trans. Ind. Electron.*, Vol. 56, No. 10, pp.4097-4106, Oct. 2009.

[4] S. Rechka, E. Ngandui, J. Xu, and P. Sicard, "A comparative study of harmonic detection algorithms for active filters and hybrid active filters," i*n Proc. PESC,* Vol. 1, pp. 357-363, June, 2002.

[5] H.Akagi, Y.Kanazawa and A. Nabae, "Instantaneous reactive power compensators comprising switching devices without energy storage components," *IEEE Trans. Ind. Appl.*, Vol. 1A-20, No. 3, pp.625-630, May/Jun., 1984.

[6] V. M. Moreno, M. Liserrre, A. Pigazo, and A. Dell'Aquila, "A comparative analysis of real-time algorithms for power signal decoposition in multiple synchronous reference frames," *IEEE Trans. Power Electron.*, Vol. 22, No. 4, pp. 1280-1289, Jul. 2007.

[7] S.D. Round and D.M.E. Ingram, "An evaluation techniques for determining active filter compensating currents in unbalanced systems," *in Proc. EPE Trondheim*, pp. 4.767-4.772, Sep. 1997.

[8] C. H. G. Santos, S. M. Silva, B. J. C. Filho, "A fourier-based PLL for single-phase grid connected systems," *in Proc. Energy Conversion Congress and Exposition (ECCE), 2010*, pp. 2626-2632, Sep. 2010.

[9] A. V. Oppenheim and A. S. Willsky, *Signals and Systems*, Prentice Hall, 2nd Ed., chap. 4, New Delhi, 2009.

[10] P. Rodriguez, L. Sainz, and J. Bergas, "Synchronous double reference frame PLL applied to a unified power quality conditioner," *in Proc. Harmonics and Quality of Power*, pp. 614- 619, Vol. 2, Oct. 2002.

[11] P. Rodriguez, "Aportaciones a los acondicionadores activos de corriente en derivación para redes trifásicas de cuatro hilos," Ph. D. Thesis, Universitat Politècnica de Catalunya, Barcelona, Jan. 2005.

[12] E. H. Watanabe, H. Akagi, and M. Aredes, "The P-Q theory for active filter control: some problems and solutions," Departament of Electrical and Electronic Engineering, Tokyo Institute of Technology, *Revista Controle & Automação,* Vol. 15, No. 1, Jan./ Mar. 2004.

[13] R. M. Santos Filho, P. F. Seixas, P. C. Cortizo, L.A.B. Torres, A. F. Souza, "Comparison of three single-phase PLL algorithms for UPS applications," *IEEE Trans. Ind. Electron.,* Vol. 55, p. 2923-2932, Aug. 2008.

[14] D. Yazdani, A. Bakhshai, G. Joos, and M. Mojiri, "A real time three-phase selective harmonic extraction approach for grid connected converters," *IEEE Trans. Ind. Electron.*, Vol. 56, No. 10, pp. 4097-4106, Oct. 2009.

Cláudio H. G. Santos was born in Divinópolis, Minas Gerais, Brazil, on May 10, 1982. He received his B.S. and M.S. in Electrical Engineering from the Federal Center of Technological Education of Minas Gerais (CEFET-MG), Minas Gerais, Brazil. He has worked as a substitute Professor at the CEFET-MG and as an auxiliary Professor at the UNA, Minas Gerais, Brazil. He is currently working as an Assistant Professor at the Federal University of Ouro Preto, João Monlevade, Brazil. His current research interests include power electronics, control systems and computational modeling.

Reginaldo V. Ferreira was born in Betim, Minas Gerais, Brazil, on August 6, 1983. He received his B.S. in Electrical Engineering from the Federal Center of Technological Education of Minas Gerais (CEFET-MG), Minas Gerais, Brazil, and specialized in Industrial Automation at the Pontifical Catholic University of Minas Gerais (PUC-MG), Minas Gerais, Brazil. He received his M.S. in Electrical Engineer at CEFET-MG. He is currently working as an Assistant Professor at the Federal Institute of Minas Gerais (IFMG), Betim, Minas Gerais, Brazil. His current research interests include power electronics, control systems and power quality systems.

Sidelmo Magalhães Silva received his B.S., M.S. and Ph.D. in Electrical Engineering from the Federal University of Minas Gerais (UFMG), Minas Gerais, Brazil, in 1997, 1999 and 2003, respectively. From October 2001 to August 2002, he worked in the Research and Development Department of ABB, Turgi, Switzerland. Since 2010, he has been working as a Professor at the Federal University of Minas Gerais. His current research interest include power quality, application of Power Electronics to power systems and hybrid vehicle powertrain technology.

Braz J. Cardoso Filho was born in Fortaleza, Brazil, on April 21, 1965. He received his B.S. and M.S. in Electrical Engineering from the Universidade Federal de Minas Gerais (UFMG), Belo Horizonte, Brazil, and his Ph.D. in Electrical Engineering from the University of Wisconsin, Madison, WI, in 1987, 1991, and 1998, respectively. Since 1989, he has held a faculty position in the Department of Electrical Engineering at the UFMG. He is a cofounder and the Director of the Industry Applications Laboratory, UFMG. He has worked in the fields of power converters, electric drives, and utility applications for power converters and is the author or coauthor of over 100 technical papers published in journals and conference proceedings. His current research interests include power electronic converters and their applications in industry and in the power grid, electric machines and drives, and power semiconductor devices.